Environmental Pollution 307 (2022) 119483

Contents lists available at ScienceDirect

Environmental Pollution

journal homepage: www.elsevier.com/locate/envpol

The interplay between atmospheric deposition and soil dynamics of mercury in Swiss and Chinese boreal forests: A comparison study☆

Chaoyue Chen [a,b,1], Jen-How Huang [g,1], Katrin Meusburger [d], Kai Li [a,b], Xuewu Fu [a,c], Jörg Rinklebe [e,f], Christine Alewell [g], Xinbin Feng [a,c,*]

[a] State Key Laboratory of Environmental Geochemistry, Institute of Geochemistry, Chinese Academy of Sciences, Guiyang, 550081, China
[b] University of Chinese Academy of Sciences, Beijing, 100049, China
[c] Center for Excellence in Quaternary Science and Global Change, Chinese Academy of Sciences, Xian, 710061, China
[d] Swiss Federal Institute for Forest, Snow and Landscape Research, 8903, Birmensdorf, Switzerland
[e] University of Wuppertal, School of Architecture and Civil Engineering, Institute of Foundation Engineering, Water and Waste Management, Laboratory of Soil and Groundwater Management, Pauluskirchstraße 7, 42285, Wuppertal, Germany
[f] International Research Centre of Nanotechnology for Himalayan Sustainability (IRCNHS), Shoolini University, Solan, 173212, Himachal Pradesh, India
[g] Environmental Geosciences, University of Basel, 4056, Basel, Switzerland

ARTICLE INFO

Keywords:
Mercury
Atmospheric deposition
Forest soil
Humus type
Podzolisation

ABSTRACT

Taking advantage of the different histories of Hg deposition in Davos Seehornwald in E-Switzerland and Changbai Mountain in NE-China, the influence of atmospheric deposition on Hg soil dynamics in forest soil profiles was investigated. Today, Hg fluxes in bulk precipitation were similar, and soil profiles were generally sinks for atmospherically deposited Hg at both sites. Noticeably, a net release of 2.07 μg Hg m^{-2} yr^{-1} from the Bs horizon (Podzol) in Seehornwald was highlighted, where Hg concentration (up to 73.9 μg kg^{-1}) and soil storage (100 mg m^{-3}) peaked. Sequential extraction revealed that organic matter and crystalline Fe and Al hydr (oxide)-associated Hg decreased in the E horizon but increased in the Bs horizon as compared to the Ah horizon, demonstrating the coupling of Hg dynamics with the podzolisation process and accumulation of legacy Hg deposited last century in the Bs horizon. The mor humus in Seehornwald allowed Hg enrichment in the forest floor (182–269 μg kg^{-1}). In Changbai Mountain, the Hg concentrations in the Cambisol surface layer with mull humus were markedly lower (<148 μg kg^{-1}), but with much higher Hg soil storage (54–120 mg m^{-3}) than in the Seehornwald forest floor (18–27 mg m^{-3}). Thus, the vertical distribution pattern of Hg was influenced by humus form and soil type. The concentrations of Hg in soil porewater in Seehornwald (3.4–101 ng L^{-1}) and in runoff of Changbai Mountain (1.26–5.62 ng L^{-1}) were all low. Moreover, the pools of readily extractable Hg in the soils at both sites were all <2% of total Hg. Therefore, the potential of Hg release from the forest soil profile to the adjacent aquatic environment is currently low at both sites.

1. Introduction

Mercury (Hg) is one of the most toxic elements and has caused concerns worldwide (UNEP, 2019). It can be transported globally due to the volatility of elemental form (Hg^0) and its long residence time (0.5–1 years) in the atmosphere (Schroeder and Munthe, 1998; Obrist et al., 2018). This allows Hg to reach remote areas without local sources (Wright et al., 2016; Wang et al., 2017). In addition, Hg in the surface environment may be transformed into methylmercury, which is a highly toxic neurotoxin that bioaccumulates in organisms and biomagnifies strongly through food chains (Beckers and Rinklebe, 2017). The higher the trophic position along food chains, the stronger biomagnification level in the organisms will be, resulting in extremely high Hg concentrations in animals or fishes, and ultimately possibly causing potential health risks to consumers (Rheinberger and Hammitt, 2012). These altogether highlight the potential health risks of Hg in the environment to plants, wild animals and humans (Lindberg et al., 2007; Gustin et al., 2020; Tsui et al., 2020).

☆ This paper has been recommended for acceptance by Wen-Xiong Wang.

* Corresponding author. State Key Laboratory of Environmental Geochemistry, Institute of Geochemistry, Chinese Academy of Sciences, Guiyang, 550081, China.
E-mail address: fengxinbin@vip.skleg.cn (X. Feng).

[1] These authors contributed equally to this work.

https://doi.org/10.1016/j.envpol.2022.119483
Received 20 February 2022; Received in revised form 12 May 2022; Accepted 13 May 2022
Available online 17 May 2022
0269-7491/© 2022 Elsevier Ltd. All rights reserved.

Forests are important compartments in the global Hg biogeochemical cycle. Mercury enters into forest ecosystems through wet precipitation and dry deposition, including foliar uptake, particulate-bound Hg and gaseous oxidised Hg deposition (Grigal, 2002; Zhang et al., 2016). Catchment studies in different forest ecosystems in Europe, USA and China have indicated retention of 76–95% of atmospherically deposited Hg in the forest soil (Grigal et al., 2000; Schwesig and Matzner, 2000; Demers et al., 2007; Fu et al., 2010). Forest soils are therefore regarded as an effective sink for atmospheric Hg (Agnan et al., 2016). Mercury has a strong affinity for organic matter, especially organic thiols, and thus high concentrations of Hg in soils are frequently accompanied by high organic carbon values (O'Driscoll et al., 2011; Obrist et al., 2011; Guedron et al., 2013). Oxide and clay minerals are the second major sorbents of Hg next to organic matter (Gabriel and Williamson, 2004; Devai et al., 2005; Beckers and Rinklebe, 2017).

To date, few studies have focused on Hg mobility and transport along the soil profile. Only some investigations have shown the vertical distribution of Hg along the profile of Cambisols, Umbrisols, Phaeozems, Fluvisols, Luvisols and Arenosols (Richardson et al., 2013; Rozanski et al., 2016; Richardson et al., 2017; Gomez-Armesto et al., 2020b). Among all soils, Podzol is one of the most investigated profiles. Based on the significant correlations between Hg, Fe and organic matter contents, podzolisation was hypothesised, but not yet proven, to transfer organic-matter-bound Hg in the forest floor through the E horizon into the Bs horizon (Richardson et al., 2013; Gomez-Armesto et al., 2020b). Nonetheless, how well such a hypothesis could be supported by Hg fluxes and speciation along the profile is still unknown. Moreover, speciation, mobility and the sink or source function of each horizon along the profile has seldom been investigated. This makes understanding the fate and transport of Hg along the profile and assessing the potential release of Hg from the soil profile very difficult.

Forest ecosystems in China and Switzerland have been exposed to very different Hg depositional trends. While there is continuously increasing Hg deposition in China, the deposition rate of Hg has decreased since the 1960s in Switzerland (Ross-Barraclough and Shotyk, 2003; Thevenon et al., 2011b). Decreased Hg deposition may create a potential re-mobilisation of Hg previously adsorbed in soils. In a forested catchment in Germany, the forest floor was recognised as a source for arsenic by releasing 11 times higher arsenic flux than the total deposition (Huang and Matzner, 2007). It was suggested that arsenic has accumulated in the forest floor at times of high arsenic deposition rates in the past and is now released from the forest floor after the arsenic deposition rates declined. In the case of Hg^0, it has been evidenced that the soil acts as Hg sinks at elevated atmospheric Hg^0 exposure and switches to sources when atmospheric Hg^0 at low levels (Xin and Gustin, 2007; Agnan et al., 2016). Our two investigated sites, Davos Seehornwald, Switzerland and Changbai Mountain, China are located within the boreal zone with similar climate conditions. Due to the different Hg deposition histories, we hypothesise that the soil dynamics along the forest soil profile could be very different between these two sites. Therefore, we aimed to understand how different histories of Hg deposition affect Hg behaviour in forest soils. More specifically, the objectives of this study were (1) to understand the sink or source function of the forest soils for Hg under current atmosphere deposition, (2) to examine whether the different Hg deposition histories in Switzerland and China may be reflected by Hg distribution and speciation along the soil profile, (3) to reveal the factors regulating Hg distribution along the soil profile and (4) to assess the potential of Hg release from the forest soils in Switzerland and China to the adjacent environment.

2. Materials and methods

2.1. Site description

The Davos Seehornwald site is located at 46°48′55.2″ N, 9°51′21.3″ E at 1639 m a.s.l. in the middle range of the subalpine belt in the eastern part of the Swiss Alps (Fig. S1a). The average annual temperature in this region is 3.4 °C, and the average annual precipitation is 1000 mm (Etzold et al., 2011). The coniferous forest is dominated by Norway spruce (Picea abies (L.) Karst.) with a maximum canopy height of 27 m and a leaf area index of about 3.9 $m^2\ m^{-2}$. The tree age of the dominant trees ranges between 250 and 400 years. The understory vegetation is rather patchy, covering roughly 30% of the forest floor and is mainly composed of dwarf shrubs and mosses. The soil types are Chromic Cambisols and Rustic Podsols (Etzold et al., 2011).

The forest catchment of Mountain Changbai (42°24′ N, 128°28' E, 6 ha) has a 600–2000 m a.s.l. altitude (Fig. S1b). The sampling sites are located at 800 m a.s.l. in a temperate mixed forest. The climate is controlled by a moist temperate continental mountain climate, with a mean annual temperature of 3.6 °C and mean annual precipitation of approximately 700 mm. The vegetation in the reserve is vertically classified into three spectra: mixed forest (600–1100 m a.s.l.), coniferous forest (1100–1700 m a.s.l.) and mountain birch zone (1700–2000 m a.s.l.). The mixed forest is dominated by *Pinus koraiensis, Quercus mongolica, Acer mono* and *Tilia amurensis*. The forest has two vertical structures (the arborous layer and shrub layer) with a canopy height of 20–30 m and canopy coverage of 80%. The coniferous forest is dominated by *Pinus koraiensis*. The birch zone is dominated by *Betula ermanii, Abies nephrolepis and Picea jezoensis* var. *komarovii*. The forest soil is mainly Haplic Cambisol (Han et al., 2018).

2.2. Bulk precipitation and throughfall sampling in Davos Seehornwald and Changbai Mountain

Bulk precipitation, throughfall and soil solutions were sampled biweekly from September 2018 to September 2019 in Seehornwald. Bulk precipitation and throughfall were collected with amber borosilicate collectors (177 cm^2) in brown glass bottles placed 1 m above the ground. A fine sieve made of glass wool filtered out needles and other litter. To minimise the probable Hg transformation during storage in the field, samplers were placed in dark tubes to avoid any impact of sunlight and spiked with 1 mL of 69% w/w HNO_3 in advance. Bulk precipitation was collected by three samplers at an open site. For throughfall sampling, six samplers were installed in a line and pooled to yield three samples for analysis at each sampling date. In Changbai Mountain, three stainless steel rain collectors with Teflon coating (1 m^2) were installed in the open field and under the canopy to retrieve bulk precipitation and throughfall during and immediately after each rain event from September 2018 to September 2019, respectively. At the end of each month, all samples were pooled together for Hg analysis. Generally, all water samples at both sites were completely oxidised with bromine chloride (BrCl) and then reduced with $SnCl_2$. The produced Hg^0 was purged from the water samples at a flow rate of 2.5 L min^{-1} by a vacuum pump and captured by a chlorine-impregnated activated carbon (ClC) trap. Mercury collected in the ClC trap was then thermally desorbed in argon carrier gas and preconcentrated into a 40% mixed acid solution (V_{HNO3}: V_{HCl} = 2 : 1). Ultimately, Hg in bulk precipitation and throughfall was calculated by Hg content in the trapping solution. More detailed protocols have been described in Li et al. (2019).

2.3. Soil solution sampling in Davos Seehornwald and runoff sampling in Changbai Mountain

Forest floor percolates were collected bi-weekly below the Oi litter layer or in the Oe humus horizon (defined as 0 cm of depth) using a zero-tension lysimeter with Plexiglas plates. In the mineral soil horizons, samples were collected at three depths (15, 50 and 80 cm) using a tension lysimeter with ceramic cups (high flow porous ceramic cups, Soil moisture Equipment Corp. Santa Barbara, USA). A vacuum of 50 kPa was applied to the tension lysimeters at the beginning of each sampling period. To account for the spatial variability below the canopy cover, eight depth replicates were installed for both types of lysimeters (the

zero-tension and tension lysimeter). The lysimeter plates and suction lysimeters had been installed and sampled in the field for more than 20 years in Seehornwald before the beginning of Hg measurements, and thus potential Hg-adsorbing surfaces were assumed to be saturated. Runoff was sampled monthly at the weir of the Baihe (Fig. S1b) in Changbai Mountain from September 2018 to September 2019. After returning to the lab, the treatment of forest floor percolate, soil solution and runoff samples were the same as bulk precipitation and throughfall (Section 2.2). The design of sampling systems and programs in field were somehow different between Seehornwald and Changbai Mountain due to different climate, topography, vegetation coverage, local laws and facilities available. In Changbai Mountain, soil porewater was not taken for Hg analysis due to the adsorption problem of Hg to the lysimeter surfaces, which were installed in 2018. Since Changbai Mountain had the highest Hg deposition recently, Hg enrichment and mobilisation in the deeper horizons were not expected (Fig. 1a). Previous investigations also showed that the distribution of Hg in the mineral soil was all similar along the profiles with different forest types in China (Zhou et al., 2017; Du et al., 2019; Ma et al., 2022). Therefore, sink functions are all expected here and we estimated the soil profile function in a more reliable way with runoff data.

2.4. Litterfall and soil sampling

Litterfall in Seehornwald was collected using twenty circular traps, installed 1 m above the ground. Each litterfall trap consisted of a ring with a 0.50 m^2 collecting area, below which a net in polyester with a mesh size of 0.25 mm was fixed. From September 2018 to October 2019, litterfall was sampled biweekly or monthly in the autumn (2018), once between December 2018 and May 2019 and twice in summer 2019. In Changbai Mountain, five litter traps were placed 1 m above the ground. Each trap was made up of a polythene frame (1 m × 1 m) and a nylon mesh (2 mm). Litter falling into the traps was collected between September 2018 and October 2019. Litterfall from both sites was oven-dried at 65 °C until a mass variation of less than 0.03% in the next 8 h, weighed, ground, homogenised and stored at 4 °C before Hg analysis. Soil samples at each forest site were taken in two plots (distance more than 10 m). Since the soil is usually inhomogeneous, in each sampling plot, forest soil (about 1 kg) was taken as a mixed sample from different walls of a soil profile by the horizon and stored in polyethylene zip-type bags. Soil samples were air-dried in a cleanroom. Subsequently, the air-dried soil samples were homogenised and sieved to 2 mm with a mortar before total Hg analysis.

2.5. Calculation of Hg-fluxes

Fluxes with throughfall and bulk precipitation were calculated by multiplying the precipitation amount with the Hg concentrations on the basis of the sampling frequency. Fluxes with soil solutions were calculated by multiplying the biweekly concentrations of Hg with the biweekly vertical water fluxes simulated by the process-based soil-vegetation-atmosphere transport model LWFBrook90 (Hammel and Kennel, 2001) that was recently implemented in an R environment (Schmidt-Walter et al., 2020). LWFBrook90 is a modification of the well-known Brook90 model (Federer, 2002; Federer et al., 2003), that simulates daily transpiration, interception, soil and snow evaporation, streamflow and soil water fluxes through a soil profile covered with vegetation. The Penman-Monteith equation modified according to Shuttleworth was used to calculate the soil and plant interception, evaporation and transpiration fluxes in the model. The values for the movement of water in the ground resulted from the numerical solution of the Richards equation. The daily meteorological forcing data was derived from the adjacent MeteoSwiss Station Davos (Seehornwald). Transport in the vadose zone was solved via the Mualem-van Genuchten model (van Genuchten, 1980). The hydraulic parameters needed to describe the water retention curve were derived from measured soil texture, bulk density and organic matter content in each soil horizon using the pedotransfer function of Puhlmann and von Wilpert (2011). Mercury fluxes with litterfall were calculated by multiplying the concentrations with the amount of litterfall based on the sampling frequency.

2.6. Sequential extraction of mercury in the forest floor and mineral soil

Mercury in the forest floor (Oe and Oa layers in Davos Seehornwald) was fractionated based on DiGiulio and Ryan (Digiulio and Ryan, 1987). Around 2.0 g of the forest floor were taken for sequential extraction, including the following five steps: (1) 25 mL of de-ionised water at 22 °C for 1 h (water-soluble fraction), (2) 25 mL of 1 M NH_4OAc 22 °C for 1 h (exchangeable fraction), (3) soluble fraction (fulvic bound) and (4) precipitates (humic bound) of 1 M NH_4OH extraction (45 mL) for 1 h with subsequent HCl acidification to pH 1 (fulvic bound) as well as (5) residual phases (*aqua regia* digestion). Around 2.0 g of the mineral soil in Seehornwald (Ah, E, Bs and C horizons) and from Changbai Mountain (Ah1 (0–5 and 5–10 cm deep), Ah2, Bw, BwC and C horizons) were taken for sequential extraction modified from Huang and Kretzschmar (2010), including the following seven steps: (1) 20 mL of de-ionised water for 1 h (water-soluble fraction), (2) 20 mL of 1 M NH_4OAc for 1 h

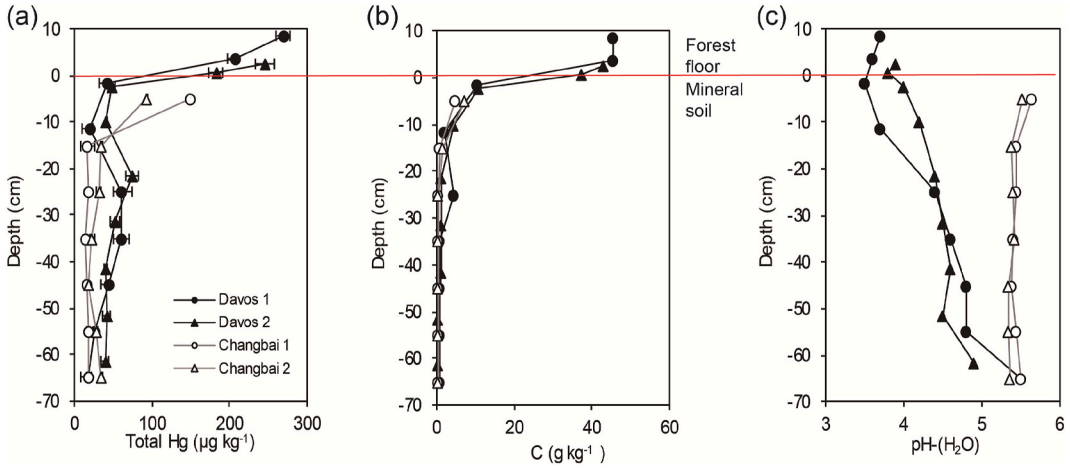

Fig. 1. (a) Concentrations of total mercury (mean ± sd), (b) carbon and (c) soil pH-(H_2O) along the soil profiles in Davos Seehornwald, Switzerland and Changbai Mountain, China; mean values and standard deviations of three replicates of total mercury concentrations are shown and standard deviations of some values are too small to be shown.

(exchangeable fraction), (3) 20 mL of 0.1 M pyrophosphate for 1 h (humic and fulvic bound), (4) 20 mL of 0.4 M $NH_2OH{\cdot}HCl$ for 0.5 h (Mn oxides), (5) 40 mL of 0.2 M NH_4-Oxalate buffer (pH 3.25) in the dark for 2 h (amorphous Fe and Al (hydr)oxides), (6) 20 mL of 4 M HCl at 95 °C for 1 h (crystalline Fe and Al (hydr)oxides) and (7) residual phases (*aqua regia* digestion). Generally, all extraction steps were performed at room temperature if not otherwise specified. After each extraction step, the suspension was centrifuged at 4000×*g* for 10 min and then decanted. The remaining soil solid was washed twice with deionised water before the next extraction step. The supernatants were filtered to 0.22-μm (PTFE Syringe Filter) for total Hg analysis.

2.7. Quality control and analysis of total mercury

Total Hg concentrations in bulk precipitation, throughfall, soil solution and supernatant samples were analysed via BrCl oxidation followed by stannous chloride reduction and dual amalgamation combined with cold vapour atomic fluorescence spectroscopy (CVAFS, Model III, Brooksrand, USA) following USEPA Method 1631 E (USEPA, 2002). The limits of detection for total Hg in aqueous samples were 0.20 ng L^{-1}. Recoveries of matrix spikes for total Hg in all liquid samples ranged between 90 and 112%. Total Hg concentrations in litterfall and soil samples were measured by a Milestone DMA-80 direct Hg analyser. National Institute of Metrology (NIM) solid standard reference materials GBW07405 (GSS-5, Yellow-red Soil: Hg: 290 ± 40 ng g^{-1}) and GBW10020 (GSB-11, Quince Leaves: Hg: 150 ± 25 ng g^{-1}) were used for soil and vegetation Hg standards, yielding recoveries of 93–110% (n = 13) and 95–108% (n = 15), respectively. The average relative standard deviation of Hg repeated analysis was 4.6%.

3. Results and discussion

3.1. Mercury in bulk precipitation, throughfall and litterfall

During the period of investigation, the concentrations of Hg in bulk precipitation were 4.26–46.4 ng L^{-1} and 4.10–33.5 ng L^{-1} in Seehornwald and Changbai Mountain, respectively (Table 1). In Switzerland, Hg deposition has declined for decades due to the strict European regulation of anthropogenic Hg emission (Ross-Barraclough and Shotyk, 2003; Thevenon et al., 2011a). However, despite the current high industrial Hg emission in China (Streets et al., 2011; Liu et al., 2019), the Hg levels in bulk precipitation in Changbai Mountain and Seehornwald were surprisingly similar. Generally, Hg concentrations in bulk precipitation in China decrease from south to north (Guo et al., 2008; Wan et al., 2009; Wang et al., 2009; Fu et al., 2010), and Changbai Mountain is located in northeastern China. In addition, Changbai Mountain is a rather remote area, being 300 km from the nearest industrial area in Changchun City (Fig. S1b), thereby explaining the low Hg concentrations in bulk precipitation.

The concentrations of Hg in throughfall at Seehornwald and Changbai Mountain were remarkably higher than in the corresponding bulk precipitation (Table 1). The increased Hg in throughfall was derived from atmospheric Hg previously deposited on the canopy (Rea et al., 2000; Grigal, 2002). The strong and significant correlation between Hg in bulk precipitation and throughfall in Seehornwald (slope: 1.79, r = 0.75, p = 0.01, Fig. S3a) and Changbai Mountain (slope: 1.81, r = 0.91, p < 0.01, Fig. S4a) indicated the washout effect seems to be similarly intensive at both sites since both sites have an average of 1.8 times higher Hg concentrations in throughfall than in bulk precipitation (Fig. S3a and S4a). Interestingly, Hg concentrations in litterfall were 18.3–31.8 μg kg^{-1} in Changbai Mountain and the values in Seehornwald were 3–4 times higher (67.3–111 μg kg^{-1}). It is accepted that foliage takes up atmospheric Hg mainly through the stomata, although Hg can also be immobilised via nonstomatal pathway, e.g. sorption, on the leaf surface (Ericksen et al., 2003; Stamenkovic and Gustin, 2009; Obrist et al., 2012; Laacouri et al., 2013). Physiological properties of foliage, like surface area index, stomatal density, and cuticle material, may influence Hg adsorption and absorption (Laacouri et al., 2013). The different forest types and tree species may affect Hg uptake efficiency by leaves in these two forest sites. Hg accumulation in litterfall is also subject to leaf longevity. A longer lifetime of needles in Seehornwald (Picea abies, more than 4 years) made more Hg accumulate in litterfall than in Changbai Mountain (*Pinus koraiensis*, *Quercus mongolica*, 0.5–3 years) (Fan et al., 2019; Navratil et al., 2019).

3.2. Mercury association with soil organic matter along the soil profile

Soil organic matter has been known as the major factor governing the spatial and vertical distribution of Hg in soils (Grigal, 2003; Richardson et al., 2013; Shetaya et al., 2019). In this study, the different forms of humic substances, i.e. mor humus in Seehornwald and mull humus in Changbai Mountain, substantially influenced not only the vertical distribution but also the mobility of Hg along the forest soil profile. In Changbai Mountain, the lack of a distinguishable litter layer reflects the rapid decomposition of litterfall at near-neutral pH and rapid integration of organic matter into the mineral topsoils (Ah1 horizon). Mercury had the highest concentration at 0–10 cm depths (92–148 μg kg^{-1}), and below 10 cm, the Hg concentrations were all <35 μg kg^{-1} (Fig. 1a). Such distribution, in general, agrees well with the organic carbon content and pH, which decreased from 5 to 7 g kg^{-1} to ~0.3 g kg^{-1} and from ~6 to ~5 with depth (Fig. 1b and c). Litterfall is generally the primary deposition pathway of Hg into forest soils, responsible for 64% and 75% of total Hg deposition in Seehornwald and Changbai Mountain, respectively (Table 2). This reflects that China's high atmospheric Hg emissions in the past two decades have been deposited in the form of litter, leading to enhanced Hg accumulation in surface soils (Gong et al., 2014; Wang et al., 2016). Such a conclusion relays on the fact that gaseous Hg re-emissions from the forest soils are much smaller than total Hg deposition. The distribution density of air-forest floor Hg^0 fluxes with a global database showed that Hg^0 fluxes occur most frequently at ~1.75 μg m^{-2} yr^{-1} in conifer forests (Agnan et al., 2016). Also, a recent study characterised that surface-air Hg flux in a forested catchment was −2.2

Table 1
Concentrations of total mercury in bulk precipitation, throughfall, litterfall, forest floor percolate, mineral soil solution and runoff from September 2018 to September 2019 in Davos Seehornwald, Switzerland and Changbai Mountain, China.

Compartment	Swiss Davos Seehornwald			Chinese Changbai Mountain		
	Median	Average	Min–Max	Median	Average	Min–Max
Bulk precipitation (ng L^{-1})	11.2 [a]	14.1	4.26–46.4	10.9[e]	14.0	4.10–33.5
Throughfall (ng L^{-1})	31.8 [a]	41.0	2.79–92.8	33.8[e]	37.9	16.1–78.3
Litterfall (μg kg^{-1})	87.7 [b]	85.1	67.3–111	26.7[f]	25.6	18.3–31.8
Forest floor percolate (ng L^{-1})	20.7 [c]	28.0	5.46–101	–	–	–
15 cm deep soil solution (ng L^{-1})	9.64 [d]	12.1	3.40–27.6	–	–	–
50 cm deep soil solution (ng L^{-1})	23.2 [a]	24.0	3.77–46.8	–	–	–
80 cm deep soil solution (ng L^{-1})	11.2 [e]	20.2	6.28–64.0	–	–	–
Runoff (ng L^{-1})	–	–	–	3.22[e]	3.23	1.26–5.62

–: not determined; sample size: a: 15; b: 8, c: 16; d: 14, e: 12. f: 9.

Table 2
Annual fluxes (mean ± sd) [a] of total mercury by bulk precipitation, throughfall, litterfall, total deposition (calculated as throughfall + litterfall) and forest floor percolate, as well as 15, 50 and 80-cm-layer soil solutions from September 2018 to September 2019 in Davos Seehornwald, Switzerland and runoff in Changbai Mountain, China.

Compartment	Swiss Davos Seehornwald (μg Hg m^{-2} yr^{-1})			Chinese Changbai Mountain (μg Hg m^{-2} yr^{-1})		
Bulk precipitation	8.02	±	0.25	5.14	±	0.02
Throughfall	19.6	±	1.01	9.55	±	0.04
Litterfall	25.0	±	0.28	15.3	±	0.69
Total deposition [b]	39.2	±	0.73	20.4	±	0.84
Forest floor percolate (a sink) [c]	19.2	±	0.67 (- 20.00 ± 0.70) [d]		–	
15-cm-deep soil (a sink) [c]	7.45	±	0.41 (- 11.75 ± 0.54) [d]		–	
50-cm-deep soil (a source) [c]	9.52	±	0.45 (+2.07 ± 0.43) [d]		–	
80-cm-deep soil (a sink) [c]	5.10	±	0.27 (- 4.42 ± 0.36) [d]		–	
Runoff		–		0.46	±	0.00

–: not available.
[a] Sds are calculated according to standard deviations of Hg concentrations measured in the spatial replicates of samples.
[b] Total deposition is calculated as the sum of throughfall and total litterfall.
[c] Represents the source or sink function of the soil horizon.
[d] Net Hg fluxes calculated as the Hg output minus input of the soil horizon.

μg m^{-2} yr^{-1}, accounting for 6.6% of the total Hg deposition (Eckley et al., 2021). Using the estimated global database, the air-forest floor Hg exchange flux was 4% and 8% of total Hg deposition in Seehornwald and Changbai Mountain, respectively.

The forest floor in Seehornwald and Ah1 horizon in Changbai Mountain are both the uppermost layers directly trapping Hg deposited from the atmosphere. Noticeably, Hg concentrations in the Seehornwald forest floor (182–270 μg kg^{-1}) were almost double those in the Ah1 horizon in Changbai Mountain (92–148 μg kg^{-1}). In Seehornwald, the acidic condition (pH = 3–4) caused by Norway spruce litterfall does allow the presence of a 5–10 cm thick forest floor containing the highest Hg concentrations along the profiles, which can be explained by (1) the efficient uptake of Hg^0 from the atmosphere via stomata and the dry deposition of Hg(II) and particulate Hg into needles (Barquero et al., 2019) as well as (2) the decomposition of soil organic matter, leading to enrichment of Hg in the forest floor (Hall and Louis, 2004). Our data here indicated the retention of 20.0 μg m^{-2} yr^{-1} in the forest floor (calculated as total Hg deposition minus the forest floor percolate flux), accounting for 51% of the total deposition (39.2 μg m^{-2}, Table 2). In comparison, rapid decomposition of litterfall in Changbai Mountain has led to the retention of Hg in the Ah1 horizon. Since the Ah1 horizon consisted of more than 95% mineral phases, similar Hg enrichment via decomposition of organic substances to the Seehornwald forest floor is almost negligible. On the other hand, the bulk soil density of the Ah1 horizon at Changbai Mountain (0.6–0.8 g cm^{-3}) was much higher than the Seehornwald forest floor layers (0.1 g cm^{-3}). Therefore, the total soil storage of Hg for each cubic metre in the forest floor in Seehornwald (20–25 mg m^{-3}) is much smaller than the topsoil Hg storage in Changbai Mountain (50–120 mg m^{-3}) (Fig. 2).

Differently from Changbai Mountain, the Hg concentration peaked additionally in mineral soils at 20–40 cm depths (60–74 μg kg^{-1}, Bs horizon) in Seehornwald. In comparison, Hg concentrations were mostly between 20 and 40 μg kg^{-1} above and below the Bs horizon (Fig. 1a). Podzolisation, the process of organic matter complexation and eluviating Fe and Al from the E horizon to the B horizon, has been proposed to govern Hg vertical distribution in Podzol (Richardson et al., 2013; Pena-Rodriguez et al., 2014; Gomez-Armesto et al., 2020a). Here, the coupling of Hg transport along the soil profile with podzolisation was moreover evidenced by the very different SE-based speciations of Hg in

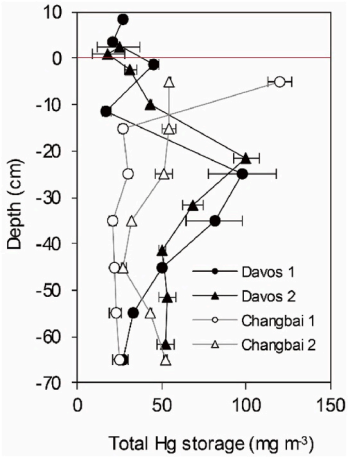

Fig. 2. Soil storage of mercury along the soil profiles in Davos Seehornwald, Switzerland and Changbai Mountain, China; mean values and standard deviations of three replicates are shown.

Ah, E, Bs and C horizons (Fig. 3b and Fig. S2b). Although fractions associated with organic matter and crystalline Fe and Al (hydr)oxides were the major components in all horizons, the concentration of organic matter associated Hg was 8.71 μg kg^{-1} in the Ah horizon, which decreased to 7.20 μg kg^{-1} in the E horizon but increased greatly to 23.0 μg kg^{-1} in the Bs horizon. A similar tendency was also observable for amorphous (0.02, 0.01 and 1.98 μg kg^{-1} in the Ah, E and Bs horizons) and crystalline Fe and Al (hydr)oxide bound Hg (26.4, 12.2 and 36.8 μg kg^{-1} in the Ah, E and Bs horizons, respectively). Such observation agrees well with the eluviation process of sesquioxides and humic acids. Together with the results from Cambisol in Changbai Mountain whose Hg vertical distribution is mainly governed by soil organic matter, we can additionally highlight that the profile Hg distribution could have a strong linkage to soil type (Frohne and Rinklebe, 2013; Richardson et al., 2013).

3.3. Interplay between atmospheric deposition and soil dynamics of mercury

The current atmospheric deposition interacted with Hg in soil profiles in Changbai Mountain and Seehornwald in markedly different ways. While the Cambisol profiles in Changbai Mountain trapped most atmospheric deposited Hg in the surface layers, there are mobilisation and immobilisation of Hg in different layers of the Podzol profiles under current atmospheric Hg deposition in Seehornwald. Based on Hg annual fluxes, the Bs horizon currently served as a source of Hg along the profile (net release 2.07 μg m^{-2} yr^{-1}), while the other layers acted as sinks (Table 2). The lack of correlation between the Hg in throughfall and forest floor percolate (Fig. S3b) indicates partial retention of throughfall Hg and some Hg mobilisation from the forest floor. The humic substances in the forest floor are effective in trapping Hg in throughfall by possibly forming strong inner-sphere complexes with e,g, reduced sulphur groups and nano-sized β-HgS (Skyllberg et al., 2006; Manceau et al., 2015). On the other hand, plant litter has been demonstrated to release Hg to a different extent based on the tree species and water compositions (Tsui et al., 2008). The lack of significant correlations between Hg in 15, 50 and 80-cm-layer soil solutions may reflect the concentrations of Hg in 50 and 80-cm-layer soil solutions were strongly influenced by Hg mobilisation from the Bs horizon. Interestingly, a strong and significant correlation between Hg in the forest floor percolate and 15-cm-layer soil solution ($r = 0.66$, $p < 0.01$, Fig. S3c) indicates the adsorption of Hg to the Ah and E horizons is likely to be more important than re-mobilisation. Unlike most other divalent metals, Hg has its greatest extent of adsorption in acidic media (Yin et al., 1996;

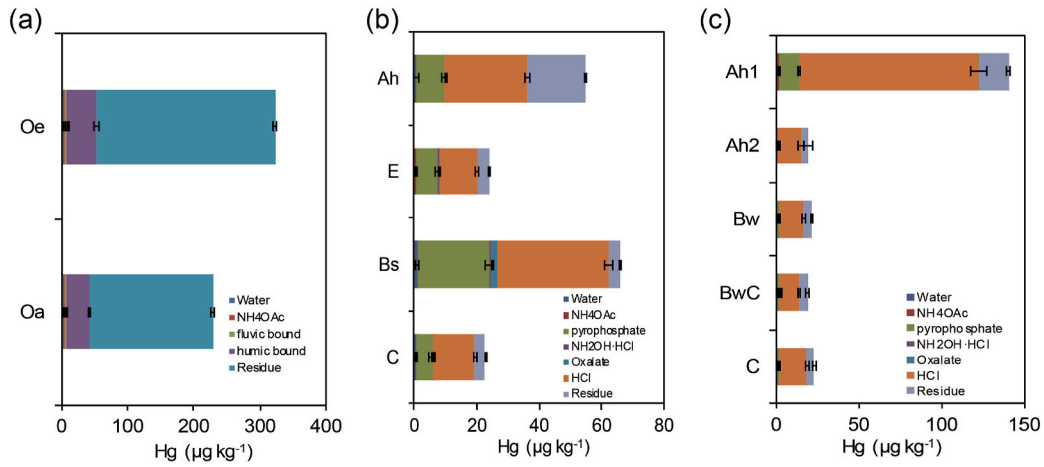

Fig. 3. Concentrations of mercury in different sequential extraction-based fractions in the (a) forest floors and (b) mineral soils in Davos Seehorwald, Switzerland and the (c) mineral soils in Changbai Mountain, China; mean values and standard deviations of three replicates are shown.

Bishop et al., 2020). In fact, stronger retention of Hg released from the upper layer was observed in the 0–15 cm layer with pH of 3.5–4.5 (62%) than in the 50–80 cm layer with pH of 4.5–5.5 (46%).

From the long-term aspect, the influence of different atmospheric deposition histories at both sites was reflected by the presence of more legacy Hg in Seehornwald profiles than in Changbai Mountain profiles. The concentrations of Hg were the lowest in the C horizon along all profiles in Seehornwald (18 and 40 μg kg^{-1}) and Changbai Mountain profiles (18 and 34 μg kg^{-1}). This reflects that the vertical distribution of Hg along the soil profiles at both sites was more likely governed by the atmospheric deposition previously rather than the geogenic source (Zheng et al., 2016). Accordingly, the accumulation of legacy Hg in Seehornwald can be reflected by (1) the much higher net total soil Hg storage in Seehornwald than in Changbai Mountain and (2) the remarkably elevated soil Hg concentrations in the Bs horizon in Seehornwald profiles. Taking the Hg level from C horizons as the baseline concentration, we estimated minimum accumulations of 0.69 and 1.78 mg m^{-2} down to 80 cm deep in the mineral soils in Davos Seehornwald, whereas 0.17 and 0.52 mg m^{-2} were estimated in Changbai Mountain (down to 70 cm deep).

A chronosequence of mineral soil Hg of Podzols in NE-USA forests has highlighted a 21–53% decrease of Hg pools in the first 20 years, but a recovery of Hg pool in 55–140 years after clear-cutting (Richardson et al., 2017). This result indicates the effective transfer and accumulation in the mineral horizons may take 30–100 years and shows that the Hg accumulated in deeper mineral horizons are legacy deposits. Indeed, mineral soil retention of Hg has been estimated on an order of centuries to millennia (Richardson and Friedland, 2015). In Davos Seehornwald, there were remarkably elevated concentrations (61–74 μg kg^{-1}) and storage levels of Hg (~100 mg m^{-3}) in the Bs horizons (20–40 cm deep) as compared to the other horizons (Figs. 1a and 2), thus showing the accumulation of legacy Hg. In comparison, the accumulation of Hg occurred exclusively in the topsoils (0–10 cm deep) in Changbai Mountain, and there was no net Hg soil storage below 10 cm deep in Changbai Mountain profiles, well reflecting its origin from the near past (Wang et al., 2013).

3.4. Potential of mercury release from forest soils and environmental implications

Generally speaking, the potential of Hg transfer in the forest soils in Seehornwald and Changbai Mountain to the adjacent aquatic environments is very low, as indicated by (1) the low Hg concentration in forest floor percolates and mineral soil solutions, (2) the very small pools of readily mobilisable Hg and (3) the effective sink function for Hg along with the mineral soil profiles. In Seehornwald, the concentration of Hg ranged from 8.97 to 25 ng L^{-1} in forest floor percolates and between 5.07 and 41 ng L^{-1} in mineral soil solutions (Table 1), which were at a similar level to those found in a remote forest in Germany (<15–131 ng L^{-1} in forest floor percolates and <15 ng L^{-1} in mineral soil solutions), (Schwesig et al., 1999). In Changbai Mountain, the Hg concentrations in runoff were also very low (1.26–5.62 ng L^{-1}).

Interestingly, the sequential extraction indicates that such a strong affinity of Hg to the forest floor and mineral soils is mostly due to the association of Hg with the recalcitrant phases (Reis et al., 2015; Morosini et al., 2021). While >80% of Hg in the forest floor was in the residual fraction, 60–95% of total Hg in Seehornwald and Changbai Mountain mineral soils was associated with crystalline and residual phases (Fig. 3 and Fig. S2). Although reductive dissolution of Fe (hydr)oxides may release Hg from mineral soils (Barringer and Szabo, 2006; Jacobson et al., 2012), the potential of large amounts of Hg mobilisation via reductive dissolution of Fe (hydr)oxides is generally scarce at both sites. This is because Hg associated with amorphous Fe and Al (hydr)oxides in mineral soils (NH_2OH·HCl and oxalate extractable fractions) is <1% in Seehornwald and <0.5% in Changbai Mountain mineral soils and crystalline Fe (hydr)oxide-bound Hg is not actively involved in redox reactions. Most Hg in the forest floor was associated with the recalcitrant fractions, e.g. the residual (>80%) and humic bound fractions (~15%, Fig. S2a). These recalcitrant fractions (>80%) possibly represent nano-particulate β-HgS component in the forest floor. Manceau et al. (2015) applied high energy-resolution X-ray absorption near-edge structure spectroscopy identifying Hg complexed to soil organic matter and nano-sized β-HgS, with fractional amounts of 26% and 74%, respectively in the O horizon of a floodplain. However, these fractions of Hg may be slowly released into aquatic environments via humic substance decomposition (Jiskra et al., 2017). The large proportion of organic matter-associated Hg (16–35% in Seehornwald and 5–11% in Changbai Mountain mineral soils, Fig. S2b and S2c), could be similarly released slowly via organic matter decomposition. In the case of the forest floor, the released Hg via oxidative decomposition will be trapped by the underlying Ah and E horizons, as evidenced by their current sink function for Hg (Table 2). The release of Hg from litter during decomposition was evidenced in a litterbag experiment carried out in an evergreen broad-leaved forest in SW-China, showing an 851% increase of water-soluble forms during one year field incubation (Yang et al., 2019). Differently from the forest floor, organic matter associated Hg released from mineral horizons will be rapidly trapped by the mineral compositions such as Fe and Al (hydr)oxide and clay minerals and the rest organo-mineral complexes, which are all effective sorbents for Hg in soils (Gabriel and Williamson, 2004; Beckers and Rinklebe, 2017).

Accordingly, there is a very low potential of Hg associated with soil organic matter being mobilised into the adjacent environments.

Another high potential release of Hg to aquatic ecosystems can be caused by the large storage of Hg in the Bs horizon. First, there were elevated Hg concentrations in 50-cm-layer porewater (21.1–41.4 ng L^{-1}) compared to 15 cm (5.07–10.5 ng L^{-1}) and 80-cm-layer porewater (9.75–32.0 ng L^{-1}, Table 1). Then, based on the calculated fluxes at different depths (Table 2), Hg along Seehornwald profiles shows a net release of 2.07 μg m^{-2} Hg from the horizon between 15 and 50 cm depths. The Bs horizon can be plausibly explained as the Hg source by its much larger Hg soil storage among all horizons (up to 100 mg m^{-3}, Fig. 2). Desorption of adsorbed Hg occurs when Hg in the solution is lower than the equilibrium concentration (Jing et al., 2008). Therefore, the legacy Hg accumulated in the past century in the Seehornwald Bs horizon may be re-mobilised due to the currently lower Hg-deposition rate than in the past century (Thevenon et al., 2011b), which lowers Hg concentrations in porewater and consequently shifts the equilibrium toward Hg desorption. This hypothesis may be reflected by the highest Hg storage but lowest Hg concentrations in porewater in the Bs horizon along the profile (Table 1 and Fig. 2). Mercury desorption from the Bs horizon seems contradicting to the fact that Hg in remote mineral soils is usually not mobile (Jiskra et al., 2017). However, our calculation indicated an annual release (2 μg Hg m^{-2} yr^{-1}) of only 0.008% of total Hg in the Bs horizon (100 mg Hg m^{-3}, 25 cm thick). Similar low desorption rates were found in batch experiments with 3 forest soils in China with Hg concentrations of 338–477 μg kg^{-1}, showing averagely desorption of 0.24–0.58% of adsorbed Hg (Xue et al., 2013). Based on the current mass balance, the net release of Hg from the Bs horizon via seepage water (2.07 μg m^{-2}) may account for approximately 5.9% of the readily mobilisable pool (35 μg m^{-2}, 15–50 cm depths). Little of the readily mobilisable pool is actually moving due to the very short equilibrium time during seepaging as compared to the extraction equilibrium (totally 2 h) in the lab. For the moment, Hg mobilisation from Bs is generally a very slow process. Moreover, the deeper horizons (50–80 cm depth) are a sink of Hg released from the Bs horizon with a net accumulation of 4.42 μg m^{-2}. Therefore, the general potential as a release of Hg into freshwaters is low. Meanwhile, such an internal transportation mechanism may significantly delay the movement of Hg downward through the soil profile and into freshwaters, increasing the lag time between atmospheric Hg deposition and its leaching to aquatic ecosystems.

A significant linear relationship between annual Hg deposition by coniferous forests and Hg concentrations in fishes within 14 ecoregions in the South Central U.S. (Drenner et al., 2013). When Hg deposition exceeds 10 μg m^{-2} yr^{-1} in coniferous forest, the average Hg concentrations in fish were suggested above the threshold concentration (300 ng g^{-1}) of Hg recommended by the U.S. EPA for the issuance of fish consumption advisories. Accordingly, total Hg deposition in Seehornwald and Changbai Mt. were 39.2 and 20.4 μg Hg m^{-2} yr^{-1}, suggesting the potential risk of over-high Hg concentrations in fishes within their aquatic ecosystem. Nevertheless, several studies with Hg concentrations in river and lake water similar to those in our soil porewater and runoff show Hg levels in fishes within the accepted guidelines of the FAO/WHO (MeHg of 3.3 μg Hg kg^{-1} $week^{-1}$) (Ramlal et al., 2003; Malczyk and Branfireun, 2015). Such contradicting statements reveal the complexity using Hg deposition rate or Hg concentrations in waters to predict Hg levels in fishes. Therefore, the transfer, transformation and bioaccumulation of Hg from the forest catchment to aquatic environments remain a cause for concern, even if the potential of Hg release from the forest soils to aquatic environments is generally low.

4. Conclusions

Unlike Hg in sediment and peatland profiles, our results reflect that Hg in the forest soil profiles does not always reflect the Hg deposition history. Depending on the soil type, the transport and accumulation of legacy Hg along the mineral profiles will be strongly coupled with the soil formation processes such as podzolisation in Seehornwald. This changes subsequently not only the vertical distribution but also the association of Hg with different solid phases in soils along the soil profile. Under current deposition rates, the soil profiles in Swiss Seehornwald and Chinese Changbai Mountain are all sinks for the atmospherically deposited Hg. Noticeably, there is a net release of Hg from the Bs horizon in Seehornwald, where the soil Hg storage is largely enriched as compared to the other mineral horizons. However, the underlying horizons retain Hg re-mobilised effectively, alleviating thus the release of Hg from the Bs horizon into the adjacent aquatic environment.

Author statement

Chaoyue Chen, Investigation, Methodology, Writing original draft, Writing – review & editing. Jen-How Huang, Investigation, Methodology, Conceptualization, Writing original draft, Writing – review & editing, Funding acquisition. Katrin Meusburger, Resources, Writing – review & editing. Kai Li, Investigation, Data curation. Xuewu Fu, Formal analysis, Conceptualization. Jörg Rinklebe, Resources, Writing – review & editing. Christine Alewell, Project administration, Writing – review & editing. Xinbin Feng, Supervision, Funding acquisition.

Declaration of competing interest

The authors declare that they have no known competing financial interests or personal relationships that could have appeared to influence the work reported in this paper.

Acknowledgements

This study was financially supported by the Natural Science Foundation of China (21661132002, 41430754), Swiss National Science Foundation (IZLCZ2_170176) and the K. C. Wong Education Foundation. We would like to appreciate Prof. Egbert Matzner (University of Bayreuth, Germany) for providing glass collector systems and Oliver Schramm, Peter Waldner, Anne Thimonier, Maria Schmitt, Beat Frey (WSL, Switzerland), Christian Simoen, Martin Gentner, Christian Rixen (SLF, Switzerland), Christian Hüglin (EMPA, Switzerland), Prof. Nina Buchmann, Philip Meier, Mana Gharun (ETH Zurich, Switzerland), Stefan Osterwalder (University of Basel, Switzerland), Andreas Kolb (University of Bayreuth, Germany) and Hao Xu (ORSCMFE, CAS, China) for their help with the field work and organisation. Many thanks are due to Claus Vandenhirtz, Kail Matuszak, Chris Kinder (University of Wuppertal, Germany) and Dr. Jianxu Wang (University of Wuppertal and SKLEG China) for the help with mercury analysis of Swiss samples.

Appendix A. Supplementary data

Supplementary data to this article can be found online at https://doi.org/10.1016/j.envpol.2022.119483.

References

Agnan, Y., Le Dantec, T., Moore, C.W., Edwards, G.C., Obrist, D., 2016. New constraints on terrestrial surface atmosphere fluxes of gaseous elemental mercury using a global database. Environ. Sci. Technol. 50, 507–524.

Barquero, J.I., Rojas, S., Esbri, J.M., Garcia-Noguero, E.M., Higueras, P., 2019. Factors influencing mercury uptake by leaves of stone pine (Pinus pinea L.) in Almaden (Central Spain). Environ. Sci. Pollut. Res. 26, 3129–3137.

Barringer, J.L., Szabo, Z., 2006. Overview of investigations into mercury in ground water, soils, and septage, New Jersey coastal plain. Water, Air, Soil Pollut. 175, 193–221.

Beckers, F., Rinklebe, J., 2017. Cycling of mercury in the environment: sources, fate, and human health implications: a review. Crit. Rev. Environ. Sci. Technol. 47, 693–794.

Bishop, K., Shanley, J.B., Riscassi, A., de Wit, H.A., Eklof, K., Meng, B., Mitchell, C., Osterwalder, S., Schuster, P.F., Webster, J., Zhu, W., 2020. Recent advances in understanding and measurement of mercury in the environment: terrestrial Hg cycling. Sci. Total Environ. 721.

Demers, J.D., Driscoll, C.T., Fahey, T.J., Yavitt, J.B., 2007. Mercury cycling in litter and soil in different forest types in the Adirondack region, New York, USA. Ecol. Appl. 17, 1341–1351.
Devai, I., Patrick, W.H., Neue, H.U., DeLaune, R.D., Kongchum, M., Rinklebe, J., 2005. Methyl mercury and heavy metal content in soils of rivers Saale and Elbe (Germany). Anal. Lett. 38, 1037–1048.
Digiulio, R.T., Ryan, E.A., 1987. Mercury in soils, sediments, and clams from a North-Carolina peatland. Water, Air, Soil Pollut. 33, 205–219.
Drenner, R.W., Chumchal, M.M., Jones, C.M., Lehmann, C.M.B., Gay, D.A., Donato, D.I., 2013. Effects of mercury deposition and coniferous forests on the mercury contamination of fish in the south central United States. Environ. Sci. Technol. 47, 1274–1279.
Du, B.Y., Zhou, J., Zhou, L.L., Fan, X.J., Zhou, J., 2019. Mercury distribution in the foliage and soil profiles of a subtropical forest: process for mercury retention in soils. J. Geochem. Explor. 205.
Eckley, C.S., Eagles-Smith, C., Tate, M.T., Krabbenhoft, D.P., 2021. Surface-air mercury fluxes and a watershed mass balance in forested and harvested catchments. Environ. Pollut. 277.
Ericksen, J.A., Gustin, M.S., Schorran, D.E., Johnson, D.W., Lindberg, S.E., Coleman, J.S., 2003. Accumulation of atmospheric mercury in forest foliage. Atmos. Environ. 37, 1613–1622.
Etzold, S., Ruehr, N.K., Zweifel, R., Dobbertin, M., Zingg, A., Pluess, P., Hasler, R., Eugster, W., Buchmann, N., 2011. The carbon balance of two contrasting mountain forest ecosystems in Switzerland: similar annual trends, but seasonal differences. Ecosystems 14, 1289–1309.
Fan, Y., Moser, W.K., Cheng, Y.X., 2019. Growth and needle properties of young pinus koraiensis Sieb. et Zucc. trees across an elevational gradient. Forests 10.
Federer, C.A., 2002. BROOK90 A Simulation Model for Evaporation, Soil Water, and Stream Flow Documentation for Versions 4 and 3.2/3/4. Compass Brook, Durham, New Hampshire.
Federer, C.A., Vorosmarty, C., Fekete, B., 2003. Sensitivity of annual evaporation to soil and root properties in two models of contrasting complexity. J. Hydrometeorol. 4, 1276–1290.
Frohne, T., Rinklebe, J., 2013. Biogeochemical fractions of mercury in soil profiles of two different floodplain ecosystems in Germany. Water, Air, Soil Pollut. 224.
Fu, X.W., Feng, X.B., Zhu, W.Z., Rothenberg, S., Yao, H., Zhang, H., 2010. Elevated atmospheric deposition and dynamics of mercury in a remote upland forest of southwestern China. Environ. Pollut. 158, 2324–2333.
Gabriel, M.C., Williamson, D.G., 2004. Principal biogeochemical factors affecting the speciation and transport of mercury through the terrestrial environment. Environ. Geochem. Health 26, 421–434.
Gomez-Armesto, A., Martinez-Cortizas, A., Ferro-Vazquez, C., Mendez-Lopez, M., Arias-Estevez, M., Novoa-Munoz, J.C., 2020a. Modelling Hg mobility in podzols: role of soil components and environmental implications. Environ. Pollut. 260.
Gomez-Armesto, A., Mendez-Lopez, M., Pontevedra-Pombal, X., Garcia-Rodeja, E., Moretto, A., Estevez-Arias, M., Novoa-Munoz, J.C., 2020b. Mercury accumulation in soil fractions of podzols from two contrasted geographical temperate areas: southwest Europe and southernmost America. Geoderma 362.
Gong, P., Wang, X.P., Xue, Y.G., Xu, B.Q., Yao, T.D., 2014. Mercury distribution in the foliage and soil profiles of the Tibetan forest: processes and implications for regional cycling. Environ. Pollut. 188, 94–101.
Grigal, D.F., 2002. Inputs and outputs of mercury from terrestrial watersheds: a review. Environ. Rev. 10, 1–39.
Grigal, D.F., 2003. Mercury sequestration in forests and peatlands: a review. J. Environ. Qual. 32, 393–405.
Grigal, D.F., Kolka, R.K., Fleck, J.A., Nater, E.A., 2000. Mercury budget of an upland-peatland watershed. Biogeochemistry 50, 95–109.
Guedron, S., Grangeon, S., Jouravel, G., Charlet, L., Sarret, G., 2013. Atmospheric mercury incorporation in soils of an area impacted by a chlor-alkali plant (Grenoble, France): Contribution of canopy uptake. Sci. Total Environ. 445, 356–364.
Guo, Y.N., Feng, X.B., Li, Z.G., He, T.R., Yan, H.Y., Meng, B., Zhang, J.F., Qiu, G.L., 2008. Distribution and wet deposition fluxes of total and methyl mercury in Wujiang River Basin, Guizhou, China. Atmos. Environ. 42, 7096–7103.
Gustin, M.S., Bank, M.S., Bishop, K., Bowman, K., Branfireun, B., Chetelat, J., Eckley, C. S., Hammerschmidt, C.R., Lamborg, C., Lyman, S., Martinez-Cortizas, A., Sommar, J., Tsui, M.T.K., Zhang, T., 2020. Mercury biogeochemical cycling: a synthesis of recent scientific advances. Sci. Total Environ. 737.
Hall, B.D., Louis, V.L.S., 2004. Methylmercury and total mercury in plant litter decomposing in upland forests and flooded landscapes. Environ. Sci. Technol. 38, 5010–5021.
Hammel, K., Kennel, M., 2001. Characterisation and Analysis of the Water Availability and the Water Balance of Forest Sites in Bavaria Using the Simulation Model BROOK90. Forstl Forschungsber München No, p. 185.
Han, D.X., Wang, N., Sun, X., Hu, Y.B., Feng, F.J., 2018. Biogeographical distribution of bacterial communities in Changbai mountain, Northeast China. Microbiologyopen 7.
Huang, J.H., Kretzschmar, R., 2010. Sequential extraction method for speciation of arsenate and arsenite in mineral soils. Anal. Chem. 82, 5534–5540.
Huang, J.H., Matzner, E., 2007. Biogeochemistry of organic and inorganic arsenic species in a forested catchment in Germany. Environ. Sci. Technol. 41, 1564–1569.
Jacobson, G.L., Norton, S.A., Grimm, E.C., Edgar, T., 2012. Changing climate and sea level alter Hg mobility at lake tulane, Florida, US. Environ. Sci. Technol. 46, 11710–11717.
Jing, Y.D., He, Z.L., Yang, X.E., 2008. Adsorption-desorption characteristics of mercury in paddy soils of China. J. Environ. Qual. 37, 680–688.
Jiskra, M., Wiederhold, J.G., Skyllberg, U., Kronberg, R.M., Kretzschmar, R., 2017. Source tracing of natural organic matter bound mercury in boreal forest runoff with mercury stable isotopes. Environ. Sci.-Proc. Imp. 19, 1235–1248.
Laacouri, A., Nater, E.A., Kolka, R.K., 2013. Distribution and uptake dynamics of mercury in leaves of common deciduous tree species in Minnesota, USA. Environ. Sci. Technol. 47, 10462–10470.
Li, K., Lin, C.J., Yuan, W., Sun, G.Y., Fu, X.W., Feng, X.B., 2019. An improved method for recovering and preconcentrating mercury in natural water samples for stable isotope analysis. J. Anal. Atomic Spectrom. 34, 2303–2313.
Lindberg, S., Bullock, R., Ebinghaus, R., Engstrom, D., Feng, X.B., Fitzgerald, W., Pirrone, N., Prestbo, E., Seigneur, C., 2007. A synthesis of progress and uncertainties in attributing the sources of mercury in deposition. Ambio 36, 19–32.
Liu, K.Y., Wu, Q.R., Wang, L., Wang, S.X., Liu, T.H., Ding, D., Tang, Y., Li, G.L., Tian, H. Z., Duan, L., Wang, X., Fu, X.W., Feng, X.B., Hao, J.M., 2019. Measure-specific effectiveness of air pollution control on China's atmospheric mercury concentration and deposition during 2013-2017. Environ. Sci. Technol. 53, 8938–8946.
Ma, H.H., Cheng, H.X., Guo, F., Zhang, L., Tang, S.Q., Yang, Z., Peng, M., 2022. Distribution of mercury in foliage, litter and soil profiles in forests of the Qinling Mountains, China. Environ. Res. 211.
Malczyk, E.A., Branfireun, B.A., 2015. Mercury in sediment, water, and fish in a managed tropical wetland-lake ecosystem. Sci. Total Environ. 524, 260–268.
Manceau, A., Lemouchi, C., Enescu, M., Gaillot, A.C., Lanson, M., Magnin, V., Glatzel, P., Poulin, B.A., Ryan, J.N., Aiken, G.R., Gautier-Luneau, I., Nagy, K.L., 2015. Formation of mercury sulfide from Hg(II)-Thiolate complexes in natural organic matter. Environ. Sci. Technol. 49, 9787–9796.
Morosini, C., Terzaghi, E., Raspa, G., Zanardini, E., Anelli, S., Armiraglio, S., Petranich, E., Covelli, S., Di Guardo, A., 2021. Mercury vertical and horizontal concentrations in agricultural soils of a historically contaminated site: role of soil properties, chemical loading, and cultivated plant species in driving its mobility. Environ. Pollut. 285.
Navratil, T., Novakova, T., Roll, M., Shanley, J.B., Kopacek, J., Rohovec, J., Kana, J., Cudlin, P., 2019. Decreasing litterfall mercury deposition in central European coniferous forests and effects of bark beetle infestation. Sci. Total Environ. 682, 213–225.
O'Driscoll, N.J., Canario, J., Crowell, N., Webster, T., 2011. Mercury speciation and distribution in coastal wetlands and tidal mudflats: relationships with sulphur speciation and organic carbon. Water, Air, Soil Pollut. 220, 313–326.
Obrist, D., Johnson, D.W., Edmonds, R.L., 2012. Effects of vegetation type on mercury concentrations and pools in two adjacent coniferous and deciduous forests. J. Plant Nutr. Soil Sci. 175, 68–77.
Obrist, D., Johnson, D.W., Lindberg, S.E., Luo, Y., Hararuk, O., Bracho, R., Battles, J.J., Dail, D.B., Edmonds, R.L., Monson, R.K., Ollinger, S.V., Pallardy, S.G., Pregitzer, K. S., Todd, D.E., 2011. Mercury distribution across 14 US forests. part I: spatial patterns of concentrations in biomass, litter, and soils. Environ. Sci. Technol. 45, 3974–3981.
Obrist, D., Kirk, J.L., Zhang, L., Sunderland, E.M., Jiskra, M., Selin, N.E., 2018. A review of global environmental mercury processes in response to human and natural perturbations: changes of emissions, climate, and land use. Ambio 47, 116–140.
Pena-Rodriguez, S., Pontevedra-Pombal, X., Gayoso, E.G.R., Moretto, A., Mansilla, R., Cutillas-Barreiro, L., Arias-Estevez, M., Novoa-Munoz, J.C., 2014. Mercury distribution in a toposequence of sub-Antarctic forest soils of Tierra del Fuego (Argentina) as consequence of the prevailing soil processes. Geoderma 232, 130–140.
Puhlmann, H., von Wilpert, K., 2011. Testing and development of pedotransfer functions for water retention and hydraulic conductivity of forest soils. Landschaftsforsch. Naturschutz 66–71.
Ramlal, P.S., Bugenyi, F.W.B., Kling, G.W., Nriagu, J.O., Rudd, J.W.M., Campbell, L.M., 2003. Mercury concentrations in water, sediment, and biota from lake Victoria, East Africa. J. Great Lake. Res. 29, 283–291.
Rea, A.W., Lindberg, S.E., Keeler, G.J., 2000. Assessment of dry deposition and foliar leaching of mercury and selected trace elements based on washed foliar and surrogate surfaces. Environ. Sci. Technol. 34, 2418–2425.
Reis, A.T., Coelho, J.P., Rucandio, I., Davidson, C.M., Duarte, A.C., Pereira, E., 2015. Thermo-desorption: a valid tool for mercury speciation in soils and sediments? Geoderma 237, 98–104.
Rheinberger, C.M., Hammitt, J.K., 2012. Risk trade-offs in fish consumption: a public health perspective. Environ. Sci. Technol. 46, 12337–12346.
Richardson, J.B., Friedland, A.J., 2015. Mercury in coniferous and deciduous upland forests in northern New England, USA: implications of climate change. Biogeosciences 12, 6737–6749.
Richardson, J.B., Friedland, A.J., Engerbretson, T.R., Kaste, J.M., Jackson, B.P., 2013. Spatial and vertical distribution of mercury in upland forest soils across the northeastern United States. Environ. Pollut. 182, 127–134.
Richardson, J.B., Petrenko, C.L., Friedland, A.J., 2017. Organic horizon and mineral soil mercury along three clear-cut forest chronosequences across the northeastern USA. Environ. Sci. Pollut. Res. 24, 27994–28005.
Ross-Barraclough, F., Shotyk, W., 2003. Millennial-scale records of atmospheric mercury deposition obtained from ombrotrophic and minerotrophic peatlands in the Swiss Jura Mountains. Environ. Sci. Technol. 37, 235–244.
Rozanski, S.L., Castejon, J.M.P., Fernandez, G.G., 2016. Bioavailability and mobility of mercury in selected soil profiles. Environ. Earth Sci. 75.
Schmidt-Walter, P., Trotsiuk, V., Meusburger, K., Zacios, M., Meesenburg, H., 2020. Advancing simulations of water fluxes, soil moisture and drought stress by using the LWF-Brook90 hydrological model in R. Agric. For. Meteorol. 291.
Schroeder, W.H., Munthe, J., 1998. Atmospheric mercury - an overview. Atmos. Environ. 32, 809–822.

Schwesig, D., Ilgen, G., Matzner, E., 1999. Mercury and methylmercury in upland and wetland acid forest soils of a watershed in NE-Bavaria, Germany. Water, Air, Soil Pollut. 113, 141–154.
Schwesig, D., Matzner, E., 2000. Pools and fluxes of mercury and methylmercury in two forested catchments in Germany. Sci. Total Environ. 260, 213–223.
Shetaya, W.H., Huang, J.H., Osterwalder, S., Mestrot, A., Bigalke, M., Alewell, C., 2019. Sorption kinetics of isotopically labelled divalent mercury (196Hg2+) in soil. Chemosphere 221, 193–202.
Skyllberg, U., Bloom, P.R., Qian, J., Lin, C.M., Bleam, W.F., 2006. Complexation of mercury(II) in soil organic matter: EXAFS evidence for linear two-coordination with reduced sulfur groups. Environ. Sci. Technol. 40, 4174–4180.
Stamenkovic, J., Gustin, M.S., 2009. Nonstomatal versus stomatal uptake of atmospheric mercury. Environ. Sci. Technol. 43, 1367–1372.
Streets, D.G., Devane, M.K., Lu, Z.F., Bond, T.C., Sunderland, E.M., Jacob, D.J., 2011. All-time releases of mercury to the atmosphere from human activities. Environ. Sci. Technol. 45, 10485–10491.
Thevenon, F., Graham, N.D., Chiaradia, M., Arpagaus, P., Wildi, W., Pote, J., 2011a. Local to regional scale industrial heavy metal pollution recorded in sediments of large freshwater lakes in central Europe (lakes Geneva and Lucerne) over the last centuries. Sci. Total Environ. 412, 239–247.
Thevenon, F., Guedron, S., Chiaradia, M., Loizeau, J.L., Pote, J., 2011b. (Pre-) historic changes in natural and anthropogenic heavy metals deposition inferred from two contrasting Swiss Alpine lakes. Quat. Sci. Rev. 30, 224–233.
Tsui, M.T.K., Blum, J.D., Kwon, S.Y., 2020. Review of stable mercury isotopes in ecology and biogeochemistry. Sci. Total Environ. 716.
Tsui, M.T.K., Finlay, J.C., Nater, E.A., 2008. Effects of stream water chemistry and tree species on release and methylation of mercury during litter decomposition. Environ. Sci. Technol. 42, 8692–8697.
UNEP, 2019. Global Mercury Assessment 2018: Technical Background Report for the Global Mercury Assessment.
USEPA, 2002. Mercury in Water by Oxidation, Purge and Trap, and Cold Vapor Atomic Fluorescence Spectrometry (Method 1631, Revision E). U.S. EPA, Washington, DC. EPA-821-R-02- 019.
van Genuchten, M.T., 1980. A closed-form equation for predicting the hydraulic conductivity of unsaturated Soils. Soil Sci. Soc. Am. J. 44, 892–898.
Wan, Q., Feng, X.B., Lu, J., Zheng, W., Song, X.J., Li, P., Han, S.J., Xu, H., 2009. Atmospheric mercury in Changbai Mountain area, northeastern China II. The distribution of reactive gaseous mercury and particulate mercury and mercury deposition fluxes. Environ. Res. 109, 721–727.
Wang, S.F., Xing, D.H., Wei, Z.Q., Jia, Y.F., 2013. Spatial and seasonal variations in soil and river water mercury in a boreal forest, Changbai Mountain, Northeastern China. Geoderma 206, 123–132.
Wang, X., Lin, C.J., Lu, Z.Y., Zhang, H., Zhang, Y.P., Feng, X.B., 2016. Enhanced accumulation and storage of mercury on subtropical evergreen forest floor: implications on mercury budget in global forest ecosystems. J. Geophys. Res.-Biogeo. 121, 2096–2109.
Wang, X., Luo, J., Yin, R.S., Yuan, W., Lin, C.J., Sommar, J., Feng, X.B., Wang, H.M., Lin, C., 2017. Using mercury isotopes to understand mercury accumulation in the montane forest floor of the eastern Tibetan Plateau. Environ. Sci. Technol. 51, 801–809.
Wang, Z.W., Zhang, X.S., Xiao, J.S., Zhijia, C., Yu, P.Z., 2009. Mercury fluxes and pools in three subtropical forested catchments, southwest China. Environ. Pollut. 157, 801–808.
Wright, L.P., Zhang, L.M., Marsik, F.J., 2016. Overview of mercury dry deposition, litterfall, and throughfall studies. Atmos. Chem. Phys. 16, 13399–13416.
Xin, M., Gustin, M.S., 2007. Gaseous elemental mercury exchange with low mercury containing soils: investigation of controlling factors. Appl. Geochem. 22, 1451–1466.
Xue, T., Wang, R.Q., Zhang, M.M., Dai, J.L., 2013. Adsorption and desorption of mercury (II) in three forest soils in Shandong Province, China. Pedosphere 23, 265–272.
Yang, G., Sun, T., An, S.W., Guo, P., Ma, M., 2019. The migration and fate of mercury during litter decomposition in a subtropical evergreen broad-leaf forest. Acta Ecol. Sin. 39 (6), 2101–2108 (In Chinese).
Yin, Y.J., Allen, H.E., Li, Y.M., Huang, C.P., Sanders, P.F., 1996. Adsorption of mercury (II) by soil: effects of pH, chloride, and organic matter. J. Environ. Qual. 25, 837–844.
Zhang, L.M., Wu, Z.Y., Cheng, I., Wright, L.P., Olson, M.L., Gay, D.A., Risch, M.R., Brooks, S., Castro, M.S., Conley, G.D., Edgerton, E.S., Holsen, T.M., Luke, W., Tordon, R., Weiss-Penzias, P., 2016. The estimated six-year mercury dry deposition across North America. Environ. Sci. Technol. 50, 12864–12873.
Zheng, W., Obrist, D., Weis, D., Bergquist, B.A., 2016. Mercury isotope compositions across North American forests. Global Biogeochem. Cycles 30, 1475–1492.
Zhou, J., Wang, Z.W., Zhang, X.S., Gao, Y., 2017. Mercury concentrations and pools in four adjacent coniferous and deciduous upland forests in Beijing, China. J. Geophys. Res.-Biogeo. 122, 1260–1274.